CSCE Annual Conference
Growing with youth – Croître avec les jeunes

Laval (Greater Montreal)
June 12 - 15, 2019

GENERATING DOWNBURST OUTFLOWS AT THE BOUNDARY LAYER WIND TUNNEL AT RYERSON UNIVERSITY

Aboutabikh, M[1,2,], Ghazal, T.[1], Aboshosha, H[1]
[1] Ryerson University
[2] maboutabikh@ryerson.ca

Abstract:

A recently developed Downburst Outflow DO-generating system at the boundary layer wind tunnel at Ryerson University is validated in this study. The system consists of multiple blades capable of suddenly changing the flow direction to generate DOs. The system is calibrated and controlled through an optimization technique developed by the authors in an earlier study to control the blade rotation and thus the resulting downbursts. The system is validated for two full-scale events at the level of mean and turbulent wind speeds both temporally and spatially. It is therefore planned to utilize the system to generate various downbursts to evaluate their effects on structures.

Keywords: Wind Tunnel, Downburst, Outflow, Thunderstorm, Gust front

1 INTRODUCTION

Downbursts are always associated with thunderstorms. During a thunderstorm event, warm air at the surface of the ground is exchanged with cooler air at higher heights. This process results into the formation of upward vertical wind motion (i.e. updrafts) and downward air motion (i.e. downdrafts). When downdrafts hit the ground, the flow is redirected radially from the point of contact with the ground causing high horizontal wind speeds, typically referred to as gust fronts. Strong downdrafts leading to high speed gust fronts are typically called downbursts. Figure 1 shows a strong downdraft (downburst) occurred near Arizona, USA in year 2016.

Figure 1: Downburst event near Arizona, USA
(https://www.eoas.ubc.ca/)

A downburst is an intensive column of air (i.e. downdraft) that induces very strong radial wind velocities (outflow) when it touches the ground (T. Fujita 1985; T. T. Fujita 1990). Those strong radial velocities typically occur at the first 50 m above the ground (T. T. Fujita and Wakimoto 1981; Oseguera and Bowles 1988; Wilson et al. 1984) which endangers low-rise structures such as transmission lines. It was reported that more than 80% of the weather-related failures of transmission lines worldwide is due to downburst events (Dempsey and White 1996; McCarthy and Melsness 1996). In Australia, downburst outflows are responsible for more than 90% of transmission line failures (Li 2000). The diameter of descending downdrafts is typically between 1000 to 6000 m (Wilson et al. 1984), and the affected high-speed zone around the downdraft is localized to 3-4 times the downdraft diameter (Aboshosha, Bitsuamlak, and El Damatty 2015; Kim and Hangan 2007; Mason, Wood, and Fletcher 2009). Studying of downbursts can be conducted by field measurements, numerically or experimentally. Examples of field measurement studies include the FAA/Lincoln Laboratory Operational Weather Studies (FLOWS) (Wolfson, DiStefano, and Fujita 1984), Northern Illinois Meteorological Research (NIMROD) and the Joint Airport Weather Studies JAWS (T. Fujita 1985). Moreover, De Gaetano et al. (2014) and Solari et al. (2012, 2015) analyzed more than 90 thunderstorm events under the “Wind and Ports” project in which an integrated system was developed based on extensive in-situ wind monitoring network, numerical simulation of wind fields, statistical analysis of wind climate, and algorithms for wind forecasting. Although field studies can

provide the actual velocity measurements, it represents a challenging task due to the uncertainty of the event occurrence location and time (localized effect). This has motivated researchers to experimentally study downbursts events (Oseguera and Bowles 1988; Lundgren, Yao, and Mansour 1992; Alahyari and Longmire 1994; Yao and Lundgren 1996; Wood et al. 2001; Chay and Letchford 2002; Elawady 2016).

Experimental modeling of downbursts can be categorized into two main groups: In Group I simulation of the entire downburst events where spatial variation is considered and Group II simulation of the downburst outflows only, where spatial variation is not considered. Group I involve the formation of the downdrafts, while Group II focuses on the effect of the outflow (after downdrafts touches down) on structures. Facilities belonging to Group I can be classified into small-scale facilities and large-scale facilities. Small-scale facilitates such as the Western Impinging Jet (Xu and Hangan 2008) are typically used to characterize the downburst wind field and not the effect of the wind on structures. That is due to the inherent constraint of simulating downburst and the structure at the same length scale where the downburst diameter is an order of magnitude greater than that of the structure. On the other hand, large-scale facilities, such as Wind Simulation and Testing (WiST) facility at Iowa State University and WindEEE dome at the University of Western Ontario for characterizing both the wind field and its effect on structures (Zhang et al. 2013; Elawady 2016; Jubayer et al. 2016).

For example, Sarkar et al. (2006) utilized WiST to model microburst events using an impinging jet and studied their effect on a tall building model using a length scale of 1:500. They compared the peak load resulting from the simulations with the loads from ASCE 7-02 assuming a synoptic wind and found out that ASCE-based peak loads are underestimated in different cases. Jesson et al. (2015) utilized the University of Birmingham Transient Wind Simulator (UoB-TWS) to simulate the primary vortex of a thunderstorm downburst and study the pressure distributions over scaled (1:1600) cube and framed structures. Jubayer et al. (2016) used the WindEEE dome facility located in the University of Western Ontario to study the response of a low rise building subjected to a simulated downburst flow. Elawady et al. (2017) performed experimental downburst simulations at the WindEEE dome on a multi-span transmission line at a length scale of 1:50. Letchford et al. (2015) used the VorTECH simulator at Texas Tech. University to model tornado vortices and study its effect on the internal pressures on a scaled low rise building model. It is worth to mention that downburst and the structure need to be simulated using the same length scale, which can be very challenging for Group I of downburst simulators as it requires a large facility (e.g., assuming a scale of 1:500 and a typical jet diameter of 1000m, simulated jet diameter (D_j) ≥ 2m with an overall radius ≥ 3 x D_j radially). In order to overcome such a challenge, researchers adopted Group II of downburst simulators where the effect of the downburst on the structure is modeled but not the downdraft formation.

For instance, Matsumoto (1984) designed a switch device with double layer louver at the outlet of the wind tunnel of atmospheric boundary layer for the investigation of the effect of downburst like wind load on trains. Lin and Savory (2006) and Lin et al. (2007) introduced a slot jet facility to simulate a downburst outflow, and successfully generated the dominant rolling vortex associated with downbursts. Butler and Kareem (2007), used two techniques to redirect the horizontal flow in a typical two-dimensional wind tunnels to generate downburst-like outflows, which augments on the existing infrastructure with minimal modifications. The implemented two techniques are: (i) A rotating flat plate with an angle varying between 0^o (i.e. horizontal) to 90^o (i.e. vertical) and (ii) A multi-fan system to alternate the flow at different elevations. Both methods created a downburst-like velocity records that match full scale data. Later, Butler et al. (2009) utilized the rotating plate technique to study downburst pressures on a prismatic square building. Zhao et al (2009) used an active control wind tunnel to introduce a sudden-increase of the wind speeds to represent the non-stationarity associated with downbursts. Although, this technique succeeded in simulating the ramping up portion of typical velocity-time variation seen in downbursts, the resulting running mean velocities (i.e. smoothed) remain constant afterwards and do not ramp down as seen in real downburst records.

Lin et al. (2012) studied the structural response of aeroelastic overhead transmission lines subjected to conventional atmospheric boundary layer and downdraft outflow through wind tunnel experiments. Downdraft outflow was simulated using a fan and a gate that was opened and shut quickly. Le and Caracoglia (2018) used a multi-blade transient flow device to simulate the downburst outflows in a traditional small-scale wind tunnel. They used a grid in the form of rectangular flat bars to simulate the turbulent flow. To model downburst profiles they used four equally spaced flat plates connected by a motor mechanism that controls the plate movement to allow the redirection of the flow. The plates are positioned horizontally first (0^o) and then angled downwards to simulate the downburst event. It was concluded that this system is suitable for downburst experimentation in conventional wind tunnels similar to the one at RU. Table 1 lists previous studies in which downburst were generated to investigate wind effect on structures.

Inspired by (K Butler and Kareem 2007; Le and Caracoglia 2018), the current study focuses on designing and calibrating a rotating blade (louver) system that allows for modeling downburst outflows. As reported by Aboshosha et al. (2017), downburst generated wind speed variation with the time can be very different (i.e single or multiple peaks) depending on the relative location of the downburst to the point of interest, jet speed and the storm translation. The blade system (or as referred to as Downburst Outflow DO-generating system) is designed to have the flexibility to generate wind speed-time variations seen in full scale downbursts. The system works with the existing wind tunnel (WT) facility at Ryerson University (RU) hand-by-hand with the recently developed Boundary Layer (BL)-generating system (Ghazal et al. 2019). Combination of the DO-generating and BL-generating systems allows for generating downburst outflows, BLs and their interaction. The DO-generating system consists of rapidly rotating blades calibrated using an aerodynamic database generated using computational fluid dynamic models (CFD), more details can be found in (Aboutabikh et al. 2019). The current study focuses on the experimental validation of the DO-generating system and is divided into 5 sections; in section 1 (this section) an introduction about downbursts and methods of generating downburst flows and/or outflows was given. Section 2 provides details about the WT, while section 3 describes the DO-generating system and the experimental setup to generate various downburst outflows. Section 4 focuses on the experimental validation using sample two full scale downburst records, while section 5 summarizes the findings and conclusions of the study.

2 WIND TUNNEL AT RU

Ryerson University (RU) currently operates a large subsonic, closed-loop WT for aerospace applications, which is sketched in Figure 2a. This wind tunnel was refurbished in 2014/2015 to improve runtime and flow quality (Barcelos 2015; Carroll 2017). The WT is equipped with a large fan that pushes air at the north side of the tunnel as shown in Figure 2a. The pushed air passes through turning vanes and then through a contraction zone to streamline the flow at the south side. The south side has a square section with dimensions of 91 x 91cm followed by a diffuser zone with dimensions varying from 91x91cm to 108x108cm as shown in Figure 2b. In our recent work, (Ghazal et al. 2019) the south section of the tunnel with the diffuser (shown in Figure 2b) was equipped with a system (shown in Figure 2c) to generate various Boundary Layers BLs (open, suburban and urban) . The BL-generating system consists of: (i) a two-layer spire-slat grid, and (ii) A number of 15 staggered 10 cm roughness blocks distributed over 6 rows. As discussed

earlier, it was decided to add the DO-generating system to the current BL-generating system to allow for simulating BL and downburst outflows separately and in-combinations if required. The location for DO-generating system was chosen to be after the roughness blocks as marked in Figure 2b and 2c.

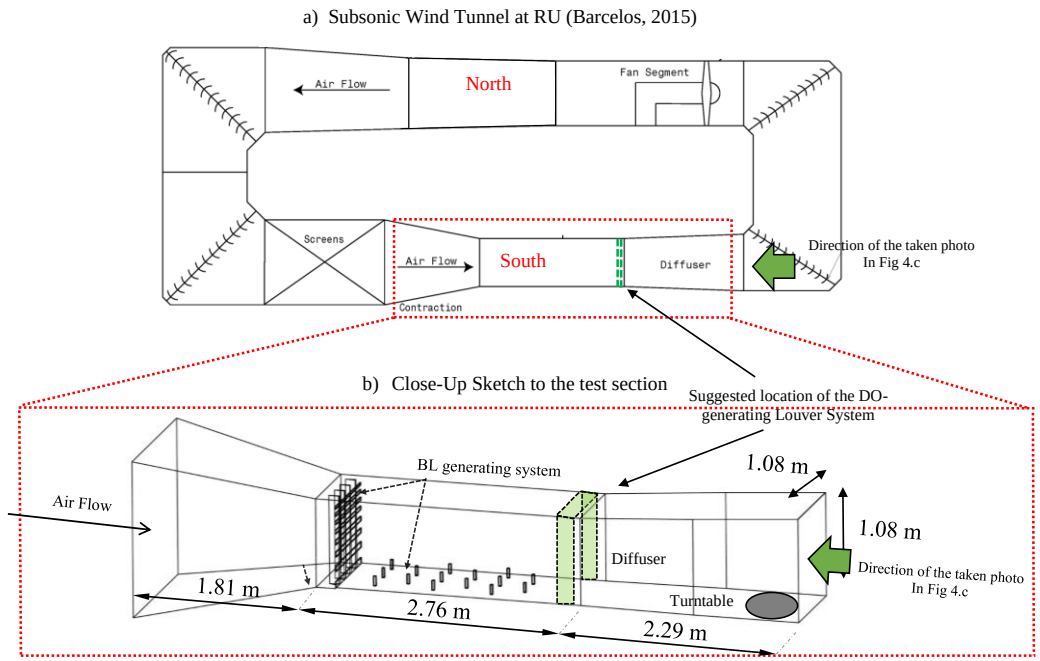

Figure 2: Wind tunnel layout and Computational model

3 EXPERIMENTAL SETUP AND DATA ANALYSIS

The DO-generating system is shown in Figure 3. The system consists of louvers that rotate as a group at an angle between -40º to +60º (measured from a horizontal line). The louvers movement is achieved using a powerful stepper motor NEMA 23, which generates a torque of up to (450 oz-in) 3.2 N.m. The motor rotation is transferred to the louver group using a rigid arm connected to a rotary cam as shown in Figure 3a. In order to maintain a minimum modification and alternation to the tunnel, the louver system and its stepper motor were kept inside the tunnel. While this may induce a negative effect on the flow quality, this was assessed and proven to be minor as will be shown in section 4. The employed louver setup is capable of rotating at a rate of 120 rpm, which means the louvers need ~0.08 sec to achieve the maximum rotation (from 0º to 60º and vice-versa). It was found out that this rotational speed is achievable for incoming wind speeds in the tunnel up to 10 m/s. As mentioned earlier, the DO-generating system works side-by side with the recently developed Boundary Layer (BL)-generating system (Ghazal et al. 2019) to simulate target downburst outflows.

The BL-generating system was set to represent an open terrain condition (Ghazal et al. 2019). The louvers were rotated according to the optimization technique developed in the previous study by Aboutabikh et al. (2019). Sample images showing louver rotation is provided in Figure 4a-c for a zero, negative, and positive angles, respectively.

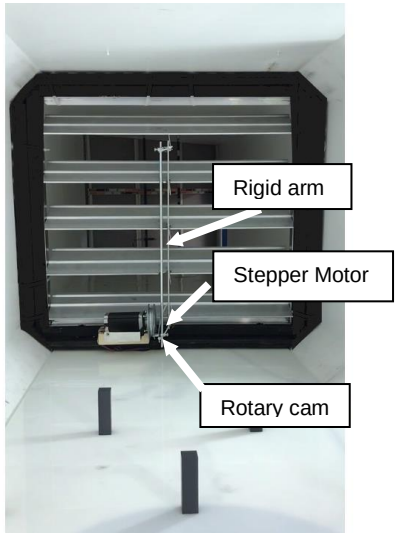

(a) Upstream view

(b) Downstream view

Figure 3: DO Generating System

(a) Do-generating system at 0^{o}

(b) Do-generating system at -30^{o}

(c) Do-generating system at +50^{o}

Figure 4: Downburst generation stages

Wind speeds at the downstream of the system (above the turntable) were characterized using 2 multi-hole pressure probes (Cobra Probes) as shown Figure 5a. Those probes operate at a sampling frequency of 1250 hz and measure the 3 velocity components within an acceptance range of ±45^{o} from the main flow direction as shown in Figure 5b. The two probes are denoted by (i) Probe A, which was fixed at a height of 0.1 m from the ground and (ii) Probe B, which was movable at different heights. Six heights were chosen for Probe B leading to a total of 7 measuring heights (0.05, 0.1, 0.20, 0.30, 0.40, 0.50 and 0.60 m) using the two probes. For each downburst test case, the test was repeated 6 times, which forms a test dataset, to cover the 6 heights of Probe B. Since this dataset was formed from non-simultaneous tests, it had to be synchronized. The synchronization was achieved using the speeds collected from Probe A, which were always recorded at a height of 0.1 m, by matching the peak of the running mean speeds. Further details about the synchronization technique can be found in Aboutabikh et al. (2019).

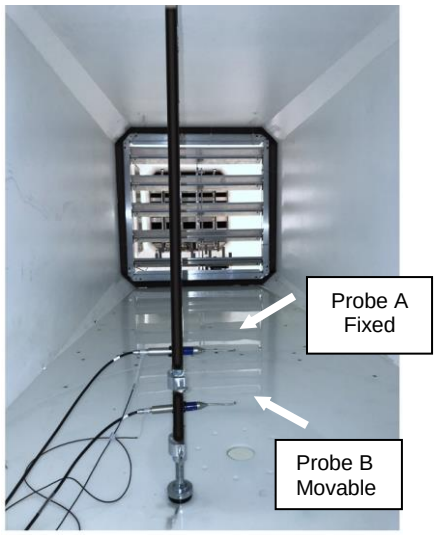

(a) Cobra Probes Used in the testing

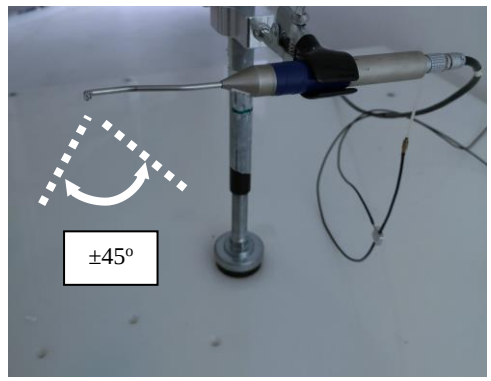

(b) Cobra Probe measuring range

Figure 5: Wind Field measurement using cobra probe devices

Wind speed recorded using cobra probes were decomposed into a running mean and a residual turbulence employing the method described by Aboshosha et al. (2015) and Elawady et al. (2017). This method applies a moving average with a time window that is equal to half the period of the main downburst vortex to extract the running mean, which is then subtracted from the total velocities to obtain the residual turbulence. Figure 6 shows sample decomposition of 2 sample wind speed records converted to the full scale (using a velocity scale of 2.6 and a length scale of 1000). As appears from the figure, the main vortex structure is always maintained in the running mean component.

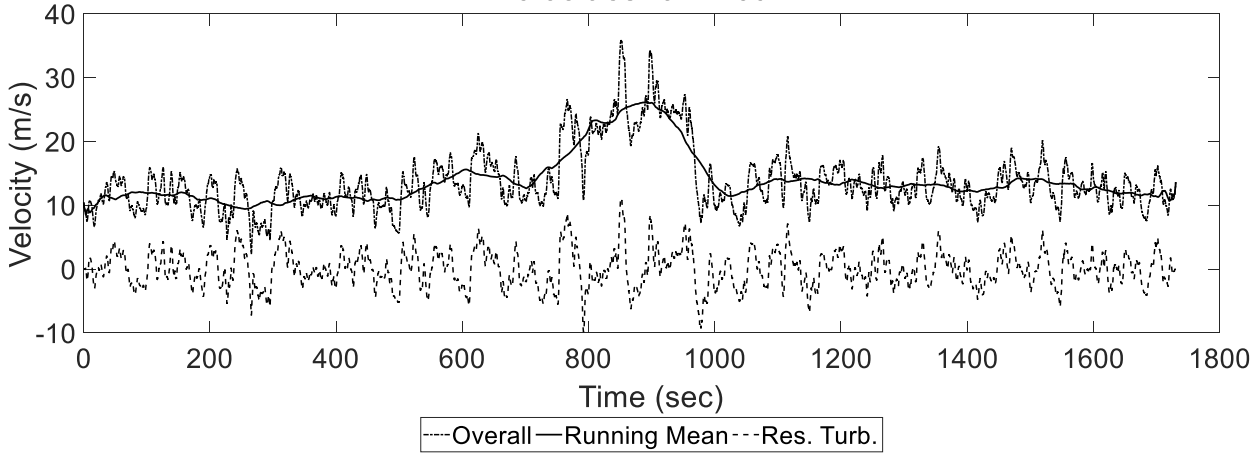

Figure 6: Validation of the DO-generating system was conducted at the following levels: (i) the temporal and spatial variations of the running mean and, (ii) characteristics of the residual turbulence Temporal and Spatial Variation of the running mean

4 VALIDATION OF THE SYSTEM

The two full scale events shown in Figure 7a,b were modeled using the DO-generating system following the blade rotation shown in Figure 7c,d. Such a blade rotation was obtained using the optimization code and aerodynamic database resulted from Aboutabikh et al. (2019). The obtained running mean velocity component from the setup is shown in Figure 7a and b in blue as well as the anticipated record from the optimization. As shown from Figures 7a and b, both the experimental-based and optimization-based mean velocities match that of the full-scale. The goodness of fitting represented by (R^2) was estimated at 90%, and 92% for the AAFB and Brisbane Airport events, respectively.

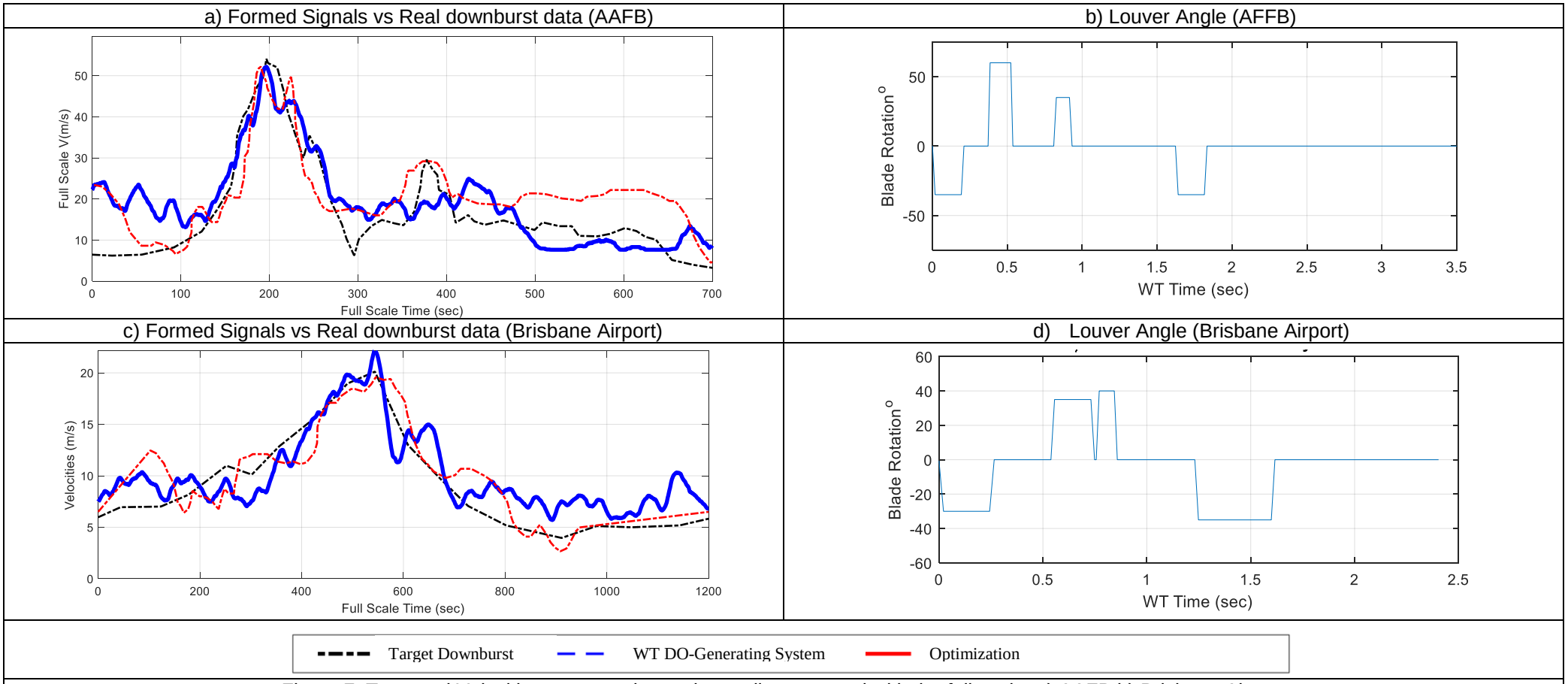

Figure 7: Temporal Velocities generated experimentally compared with the full scale: a) AAFB b) Brisbane Airport

Spatial variation of the running mean was characterized for the Reese AAFB full scale event. Wind speed data were re-collected at lower heights (0.025, 0.05, 0.01, 0.15, 0.20, 0.225 m) where the downburst outflow exists. Figure 8 shows the profile of the vertical variation of the peak running mean velocity obtained from the WT compared with the profiles of peak velocities available in the literature. It is important to note that most velocity profiles available in the literature are normalized by the jet (i.e. downdraft) diameter D_j since the actual jet diameter is known, which is not the case for our WT profile. The comparison shown in Figure 8 is based on normalizing WT profiles using an equivalent jet diameter D_{jeq}. The method suggested by Aboshosha et al. (2015, 2017) to relate the equivalent jet diameter D_{jeq} to the shedding frequency F_{sh} of the main vortex and the jet speed V_j and expressed by Equation 1 was utilized. This method led to an equivalent jet dimeter D_{jeq} of 1800 m, which was utilized in comparing WT profile with the profiles from the literature in Figure 8. As indicated from Figure 8, the DO- generating system leads to the proper vertical profile of the maximum running mean velocity.

$$D_{jeq} = \frac{V_j F_{sh}}{S_t} \qquad \text{Equation 1}$$

where V_j: jet velocity which can be taken as $V_{peak}/1.6$ for open terrain (Aboshosha et al. 2015); S_t: Strouhal number ~ 0.6; F_{sh}: shedding frequency of the main vortex =0.006hz.

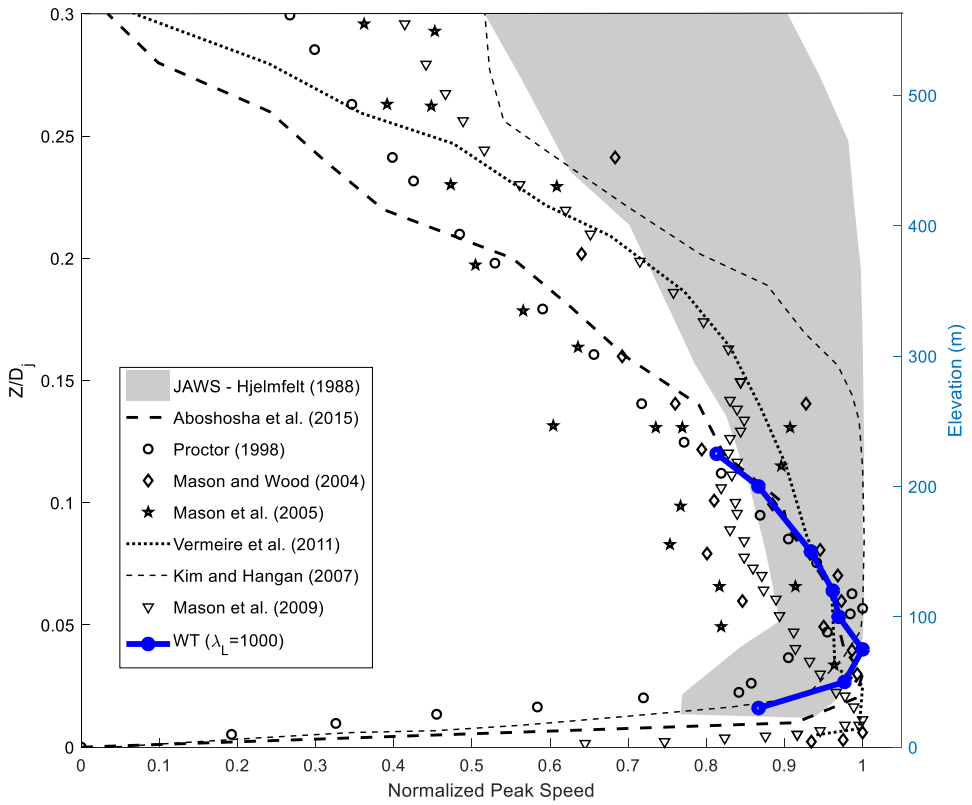

Figure 8: Vertical Profiles of the maximum running-mean speed

The turbulence intensity of downbursts is non-stationary (changes with the time). In order to overcome the challenge in the non-stationarity, the turbulence intensity was evaluated near the time instance of the main vortex. A window of $2T_{vortex}$ was used to quantify the turbulence intensity I_{max} as shown in Equation 6 (considering a quasi-stationary process).

$$I_{max=}\frac{\sigma(t)}{U_{rmax}(t)}, \quad t = T_{max} \mp T_{vortex} \qquad \text{Equation 2}$$

where σ is the rms, U_{rmax} is the maximum running mean speed, T_{max} is the time instance of the peak mean speed. T_{vortex} is the time period of the main vortex.

Figure 9 shows the vertical variation of the turbulence intensity resulting from the system. Since there is limited full scale data available for vertical profiles of the turbulence intensity (Holmes et al. 2008; Zhang et al. 2018), it was decided to compare the data with the turbulence intensity of synoptic boundary layer wind. The turbulence intensity was evaluated according to the ESDU (2010) and included in Figure 9 for comparison. The comparison shows a good match between turbulence intensities resulting from the system and from the ESDU for elevations greater than 50m. This means that turbulence intensity resulting from the system at the time instance of the maximum mean speed is compatible with the turbulence intensity of synoptic wind. A similar finding was obtained by Holmes et al. (2008). A lower turbulence intensity (i.e. 12% compared with 14%) was seen at 50m and below compared with the ESDU, which may be due to the presence of the stepper motor inside the tunnel.

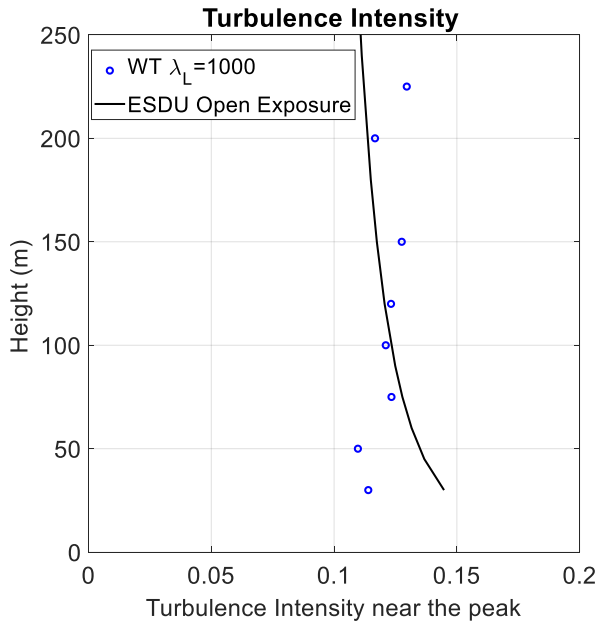

Figure 9: Vertical Profiles of the maximum speed and turbulence intensity (at the time instance of the peak)

Power spectral densities (PSD) of the residual turbulence were also evaluated and plotted as shown in Figure 10 at two sample heights. Residual turbulence near the maximum mean speed (within $\pm T_{vortex}$ from T_{peak}) was employed in generating the PSD plots. The resulting spectra were compared in Figure 10 with the spectra from ESDU (2010) considering open terrain condition (z_0=0.03 m) and the utilizing the maximum running-mean speed U_{rmax} seen in DO records. Figure 10 shows that PSD of the residual turbulence matches the PSD of the synoptic boundary layer at frequencies greater 0.012hz, which represents the cut off frequency between the running mean and residual turbulence (twice the frequency of the main vortex frequency). This agrees with the observation seen by Holmes et al. (2008).

One of the concerns of the suggested setup is the existence of potential unwanted vortices generated from the tips of the multi-blades. In order to assess the significance of those vortices, velocity spectra were evaluated at two sample heights downstream the blades as shown in Figure 10. The spectra obtained for the residual turbulence matched that of the synoptic ESDU boundary layer wind with the -5/3 slope at inertial subrange. Since there are no sharp peaks in the spectral plots, it can be concluded that blade tip vortices are negligible. The plots also show that the spectra of the running mean component is higher than the corresponding spectra for synoptic BL (ESDU) at frequencies close to the main vortex frequency (0.006 hz in this example).

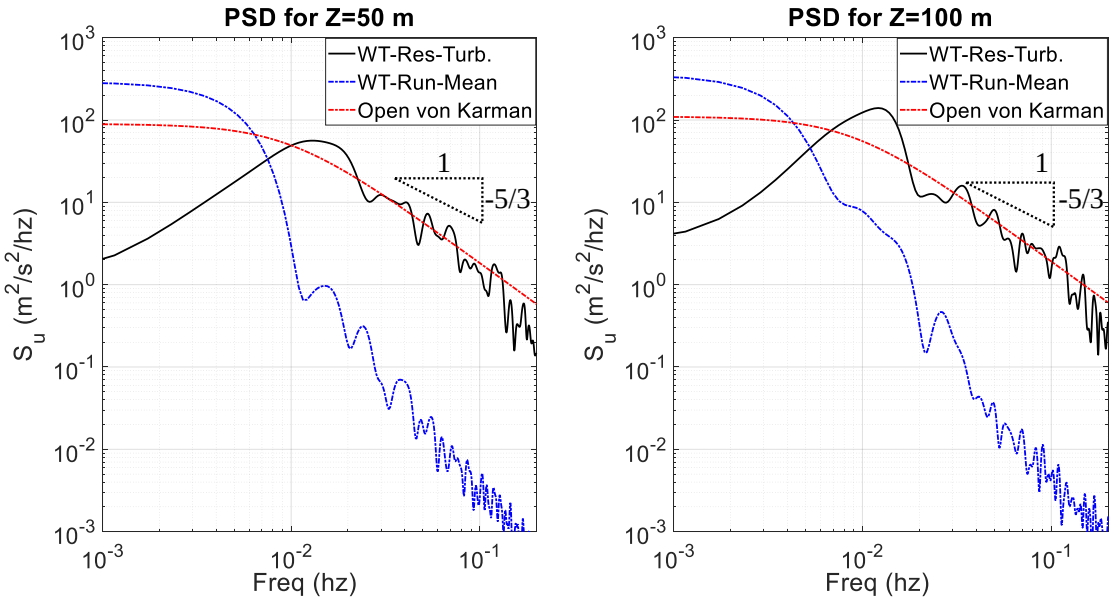

Figure 10: Spectra of the Generated Downburst velocities compared with ESDU profiles

The results presented in this section (Figures 7-10) confirm the capability of the DO-generating system to produce downburst outflows reasonably matching to those of the full scale. This include the temporal and spatial variation of the mean speeds (in the vertical direction). The system also produces the residual turbulence matching to those of the synoptic winds (when turbulence is analyzed close to the time instance of the peak).

5 CONCLUSIONS

A downburst outflow DO-generating system at RU WT is utilized to simulate full scale downbursts. The system is calibrated through an aptimization technique and a previously obtained database to identify blade rotations leading to the target downburst outflow. Two full-scale outflows were simulated in the current study employing the DO-gnerating system. The system is capable to simulate proper transient nature of the running mean wind speed component and the vertical profile of the maximum mean speeds. In addition, turbulent wind speed component at the time instance of the maximum mean speed was also analyzed and is found compatible with that of the synoptic wind. It is planned to utilize the system to generate various downburst outflows at and evaluate their effect on structures.

ACKNOWLEDGEMENT

The authors would like to thank Ryerson University for the funding of this project through the start-up and equipment grants of the last author. Also, the authors are thankful to the team at the WindEEE research institute for kindly lending the Cobra Probe system.

REFERENCE

Aboshosha, H., Bitsuamlak, G., and El Damatty, A. 2015. Turbulence Characterization of Downbursts Using LES. *Journal of Wind Engineering and Industrial Aerodynamics* 136: 44–61. https://doi.org/10.1016/j.jweia.2014.10.020.

Aboshosha, H., and Mara, T. 2018. “Estimated Wind Speeds of Thunderstorm Gust Fronts Using Historical Records and Monte Carlo Simulations.” *Journal of Wind Engineering and Industrial Aerodynamics*.

Aboutabikh, M., Ghazal, T., Chen, J., Elgamal, S., and Aboshosha, H. 2019. Designing a Blade-System to Generate Downburst out Fl Ows at Boundary Layer Wind Tunnel. *Journal of Wind Engineering & Industrial Aerodynamics* 186 (December 2018): 169–91. https://doi.org/10.1016/j.jweia.2019.01.005.

Alahyari, A, and Longmire, E K. 1994. Particle Image Velocimetry in a Variable Density Flow: Application to a Dynamically Evolving Microburst. *Experiments in Fluids* 17 (6): 434–40.

Barcelos, D. 2015. Flow Quality Testing and Improvement of the Ryerson University Low Speed Wind 14 Tunnel. Ryerson University. Ryerson University.

Butler, K, and Kareem, A. 2007. Physical and Numerical Modeling of Downburst Generated Gust Fronts. In *Proceedings of the 12th International Conference on Wind Engineering, Cairns, Australia*, 791–98.

Butler, K, Kareem, A., Cao, S., and Tamura, Y. 2009. Analysis of the Surface Pressure Characteristics of Prismatic Models in Gust Front and Downburst Outflows. In *11th Americas Conference on Wind Engineering*, 22–29.

Carroll, T. B. 2017. A Design Methodology for Rotors of Small Multirotor Vehicles. Reyrson University.

Chay, M T, and Letchford, C W. 2002. Pressure Distributions on a Cube in a Simulated Thunderstorm Downburst—Part A: Stationary Downburst Observations. *Journal of Wind Engineering and Industrial Aerodynamics* 90 (7): 711–32.

Dempsey, D, and White, H. 1996. Winds Wreak Havoc on Lines. *Transmission and Distribution World* 48 (6): 32–37.

Elawady, A. 2016. Development of Design Loads for Transmission Line Structures Subjected to Downbursts Using Aero-Elastic Testing and Numerical Modeling. Western University. https://ir.lib.uwo.ca/etd/4242/.

Elawady, A., Aboshosha, H,. El Damatty, A., Bitsuamlak, G., Hangan, H., and Elatar, A. 2017. Aero-Elastic Testing of Multi-Spanned Transmission Line Subjected to Downbursts. *Journal of Wind Engineering and Industrial Aerodynamics* 169: 194–216.

Fujita, T . 1990. Downbursts: Meteorological Features and Wind Field Characteristics. *Journal of Wind Engineering and Industrial Aerodynamics* 36: 75–86.

Fujita, T, and Wakimoto, R. M. 1981. Five Scales of Airflow Associated with a Series of Downbursts on 16 July 1980. *Monthly Weather Review* 109 (7): 1438–56.

Fujita, T. 1985. The Downburst-Micoburst and Macroburst Report of Projects NIMROD and JAWS. *Report of Projects NIMROD and JAWS*. The University of Chicago.

Gaetano, P., Repetto, M. P., Repetto, T., and Solari, G. 2014. Separation and Classification of Extreme Wind Events from Anemometric Records. *Journal of Wind Engineering and Industrial Aerodynamics* 126: 132–43. https://doi.org/10.1016/j.jweia.2014.01.006.

Ghazal, T., Chen, J., Aboshosha, H., and Sameh, E. 2019. Flow-Conditioning of a Subsonic Wind Tunnel to Model Boundary Layer Flows. *Wind and Structures*.

Jesson, M., Sterling, M., Letchford, C., and Haines, M. 2015. Aerodynamic Forces on Generic Buildings Subject to Transient, Downburst-Type Winds. *Journal of Wind Engineering and Industrial Aerodynamics* 137: 58–68.

Jubayer, C, Elatar, A., and Hangan, H. 2016. Pressure Distributions on a Low-Rise Building in a Laboratory Simulated Downburst. *8th International Colloquium on Bluff Body Aerodynamics and Applications*.

Kim, J, and Hangan, H. 2007. Numerical Simulations of Impinging Jets with Application to Downbursts. *Journal of Wind Engineering and Industrial Aerodynamics* 95 (4): 279–98.

Le, V., and Caracoglia, L. 2018. Simulating gust front downburst outflows using a multi-blade transient flow device in a small. *Journal of Wind Engineering and Industrial Aerodynamics* 3: 0–23.

Letchford, C., Levitz, B., and Darryl J. 2015. Internal Pressure Dynamics in Simulated Tornadoes. In *Structures Congress 2015*, 2689–2701.

Li, C Q. 2000. A Stochastic Model of Severe Thunderstorms for Transmission Line Design. *Probabilistic Engineering Mechanics* 15 (4): 359–64.

Lin, W E, Orf L G, Savory E, and Novacco C. 2007. Proposed Large-Scale Modelling of the Transient Features of a Downburst Outflow. *Wind and Structures* 10 (4): 315–46.

Lin, W E, and Savory E. 2006. Large-Scale Quasi-Steady Modelling of a Downburst Outflow Using a Slot Jet. *Wind and Structures* 9 (6): 419–40.

Lin, W E, Savory E, McIntyre R P, Vandelaar C S, and King, J P C. 2012. The Response of an Overhead Electrical Power Transmission Line to Two Types of Wind Forcing. *Journal of Wind Engineering and Industrial Aerodynamics* 100 (1): 58–69.

Lundgren, T S, Yao J, and Mansour, N N.1992. Microburst Modelling and Scaling. *Journal of Fluid Mechanics* 239: 461–88.

Mason, M., Graeme, S., Wood S, and Fletcher, D F. 2009. “Numerical Simulation of Downburst Winds.” *Journal of Wind Engineering and Industrial Aerodynamics* 97 (11–12): 523–39.

McCarthy, P, and Melsness, M. 1996. Severe Weather Elements Associated with September 5, 1996 Hydro Tower Failures near Grosse Isle, Manitoba, Canada. *Manitoba Environmental Service Centre, Environment Canada*, 21.

Sarkar, P, Fred L, Balaramudu V, and Sengupta, A. 2006. Laboratory Simulation of Tornado and Microburst to Assess Wind Loads on Buildings. In *Structures Congress 2006: Structural Engineering and Public Safety*, 1–10.

Solari, G., Burlando, M., De Gaetano, P. and Repetto, M. 2015. Characteristics of Thunderstorms Relevant to the Wind Loading of Structures. *Wind and Structures, An International Journal* 20 (6): 763–91. https://doi.org/10.12989/was.2015.20.6.763.

Solari, G, Repetto, M , Burlando, M., De Gaetano, P , Pizzo, M., Tizzi, M. and Parodi, M. 2012. The Wind Forecast for Safety Management of Port Areas. *Journal of Wind Engineering and Industrial Aerodynamics* 104–106: 266–77. https://doi.org/10.1016/j.jweia.2012.03.029.

Wilson, J. W, Roberts, R. D., Kessinger, C., and McCarthy, J.. 1984. Microburst Wind Structure and Evaluation of Doppler Radar for Airport Wind Shear Detection.*Journal of Climate and Applied Meteorology* 23 (6): 898–915.

Wolfson, M., DiStefano, Thomas, J., and Fujita, T. 1984. Low-Altitude Wind Shear Characteristics in the Memphis, TN Area Based on Mesonet and LLWAS Data. In *Proceedings of the 14th Conference on Severe Local Storms,*. Indianapolis: American Meteorological Society,.

Wood, G S, Kwok C., Motteram, N., and Fletcher, D. 2001. Physical and Numerical Modelling of Thunderstorm Downbursts. *Journal of Wind Engineering and Industrial Aerodynamics* 89 (6): 535–52.

Xu, Z. and Hangan, H. 2008. Scale, Boundary and Inlet Condition Effects on Impinging Jets. *Journal of Wind Engineering and Industrial Aerodynamics* 96 (12): 2383–2402. https://doi.org/10.1016/j.jweia.2008.04.002.

Yao, J, and Lundgren, T S. 1996. Experimental Investigation of Microbursts. *Experiments in Fluids* 21 (1): 17–25.

Zhang, Y., Hu, H., and Sarkar, P. 2013. Modeling of Microburst Outflows Using Impinging Jet and Cooling Source Approaches and Their Comparison. *Engineering Structures* 56: 779–93.